2014 IEEE International Conference on Fuzzy Systems (FUZZ-IEEE)
July 6-11, 2014, Beijing, China

Fuzzy Approximation Adaptive Control of Quadruped Robots with Kinematics and Dynamics Uncertainties

Zhijun Li
The Key Lab of Autonomous System and Network Control
College of Automation Science and Engineering
South China University of Technology, Guangzhou, China
Email:zjli@ieee.org

Shengtao Xiao and Shuzhi Sam Ge
Electrical & Computer Engineering Department
National University of Singapore, Singapore 117576
Email: xiao_shengtao@nus.edu.sg, samge@nus.edu.sg

Abstract*—This paper investigates optimal feet forces distribution and control of quadruped robots with uncertainties in both kinematics and dynamics. First, a constrained dynamics of quadruped robots is established. The distribution of required forces and moments on the supporting legs of a quadruped robot can be formulated as a problem for minimizing an objective function subject to form-closure constraints and balance constraints of external force. The dynamics of recurrent neural network for real-time force optimization are proposed. For the obtained optimized tip-point force and the motion of legs, we propose the hybrid motion/force control based on adaptive fuzzy system to compensate for the external perturbation and the task-space tracking errors in the environment. The proposed control can confront the uncertainties including approximation task space error and external perturbation. The verification of the proposed control is conducted using the extensive simulations.

Keywords: quadruped robot, forces distribution, external wrench, motion/force control

I. Introduction

A quadruped robot is with better mobility and able to interact with the environment through multiple contacts to maintain dynamic balance. The dynamic balance control for the walking machines is particularly important. In this respect, several research results have been reported [3], [4], [5], [6].

Force distribution problem is that each leg of walking machine supporting the body applies a certain force on the support point, which is balanced using an (equal and opposite) reaction force of the ground. The geometry of the structure and the position of the legs produce the distribution of forces and moments on the legs. Since the physical constraints producing the contact forces are only inequalities, therefore, the mathematical solution is not unique, the optimization of the force for the legs is required. Then, the force distribution problem can be formulated as a nonlinear constrained programming problem under nonlinear equality and inequality constraints.

This work is supported in part by the Foundation of Key Laboratory of Autonomous Systems and Networked Control (Chinese Ministry of Education) grant No. 2013A04, National Natural Science Foundation of China grants 61174045, the Fundamental Research Funds for the Central Universities under Grant 2013ZG0035, the Program for New Century Excellent Talents in University under Grant NCET-12-0195, and the Ph.D. Programs Foundation of Ministry of Education of China under Grant 20130172110026.

In the literature, several approaches and algorithms have been proposed to find the optimal solution of force distribution problem for legged robots. In [2], an analysis of energy efficiency was presented with respect to structural parameters, interaction forces, friction coefficient and duty factor of wave gaits, based on a simplified model of a six-legged robot. In [8], a method for optimal force distribution for the legs of a quadruped robot was presented. In [9], an approach consisting of the contact force feasibility (CFF) and the contact force distribution (CFD) for the equilibrium of a multi-contact robot was presented.

As we know, the contacts provide the required forces to maintain a quadruped robot in balance even with existence of the perturbation of external wrenches (forces and moments) including the gravity force and the inertia wrench. Since each foot is independently characterized by non-penetration and no-slip constraint with the ground, and the external wrench is usually time-varying. The contact forces must satisfy certain constraints, i.e., the friction cone constraint, and can be solved in real time to balance the varying external wrench. Therefore, how to determine the existence of feasible contact forces to resist an external wrench and maintain the systems equilibrium needs to be studied. On the other hand, for a resistable external wrench, there will be infinite solution to counterbalance it, since there are many configurations. Then some optimization criteria should be adopted in computing the contact forces, usually to minimize their overall magnitude. To perform dynamic balance control for the walking machines, the result of contact-force optimization must be used in the control law, and thus, the optimal force-distribution problem should be solved in real time.

The previous works [2], [8], [9] on multi-legged robots did not consider a detailed kinematics and dynamic behavior of the leg and trunk body, although its contribution to gait generation is significant. Most of the studies on walking robot dynamics are conducted with simplified models of legs and body. However, in order to have a better understanding of its walking, dynamics and other important issues of walking, such as dynamic stability, and its on-line control, kinematics

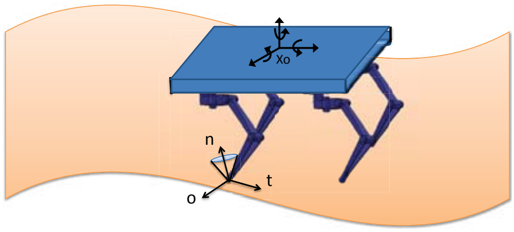

Fig. 1: A quadruped robot

and dynamic models based on a walking robot design are necessary. To the best of the authors knowledge, no significant study is reported on integrating contact force optimization and dynamic stability of a quadruped robot.

II. Dynamics of a Quadruped Robot

A. Leg Dynamics

Consider ith 3-DOF leg of a quadruped robot shown in Fig. 1, the dynamics of the system can be expressed in the vector-matrix form as given below

$$M_i(q_i)\ddot{q}_i + C_i(q_i, \dot{q}_i) + G_i(q_i) = \tau_i - J_{gi}^T F_{gi} + J_{ei}^T F_{ei} \quad (1)$$

where q_i is the 3×1 joint position vector, $M_i(q_i)$ is the 3×3 mass matrix of the leg, $C_i(q_i, \dot{q}_i)$ is a 3×1 vector of centrifugal and Coriolis terms, $G_i(q_i)$ is a 3×1 vector of gravity terms, τ_i is the 3×1 vector of joint torques, J_{ei} is the Jacobian matrix from the connect point of legs to the joint space, F_{ei} is the coupled force between the legs and the body, J_{gi} is the Jacobian matrix related to the ground reaction forces, and $F_{gi} = [f_{ix}, f_{iy}, f_{iz}]^T$ is the 3×1 vector of ground reaction forces of ith leg. During the leg's swing phase, there is no foot-terrain interaction, and F_{gi} becomes equal to zero. However, during the support phase, the ground contact exists. For multi-contact of the robot, F_{gi} becomes undetermined, which has to be solved using an optimization criterion, e.g., optimal feet forces' distributions.

The dynamics of k legs can be expressed concisely as

$$M(q)\ddot{q} + C(q, \dot{q})\dot{q} + G = \tau - J_g^T F_g + J_e^T F_e \quad (2)$$

where $M(q)$ = block diag $[M_1(q_1), \ \ldots, \ M_k(q_k)] \in R^{3k \times 3k}$; $q = [q_1, \ \ldots, \ q_k]^T \in R^{3k}$; $\tau = [\tau_1^T, \ \ldots, \ \tau_k^T]^T \in R^{3k}$; $G = [G_1^T, \ \ldots, \ G_k^T]^T \in R^{3k}$; $F_e = [F_{e1}^T, \ \ldots, \ F_{ek}^T]^T \in R^{3k}$; $F_g = [F_{g1}^T, \ \ldots, \ F_{gk}^T]^T \in R^{3k}$; $C(q, \dot{q})$ = block diag $[C_1(q_1, \dot{q}_1), \ \ldots, \ C_m(q_k, \dot{q}_k)] \in R^{3k \times 3k}$; J_g^T = block diag $[J_{g1}^T, \ \ldots, \ J_{gk}^T]^T \in R^{3k \times 3k}$, J_e^T = block diag $[J_{e1}^T, \ \ldots, \ J_{ek}^T]^T \in R^{3k \times 3k}$.

B. Body Dynamics

Let $x_o \in R^{n_o}$ the position/orientation vector of the body, the equation of motion of the quadruped robot body is written by the resultant force vector $F_o \in R^{n_o}$ acting on the center of mass of the body, the symmetric positive definite inertial matrix $M_o(x_o) \in R^{n_o \times n_o}$ of the body, the Corioli and centrifugal matrix $C_o(x_o, \dot{x}_o) \in R^{n_o \times n_o}$, and the gravitational force vector $G_o(x_o) \in R^{n_o}$ as

$$M_o(x_o)\ddot{x}_o + C_o(x_o, \dot{x}_o)\dot{x}_o + G_o(x_o) = F_o \quad (3)$$

Define $J_o(x_o) \in R^{3k \times n_o}$ as $J_o(x_o) = [J_{1o}^T(x_o), \ \ldots, \ J_{ko}^T(x_o)]^T$ with the Jacobian matrix $J_{io}(x_o)$ from the body frame $O_o X_o Y_o Z_o$ to the ith leg frame $O_{ie} X_{ie} Y_{ie} Z_{ie}$. Then F_o can be written as $F_o = -J_o^T(x_o)F_e$. Given the resultant force F_o, the leg support force F_e can be represented by $F_e = -(J_o^T(x_o))^+ F_o$, where $(J_o^T(x_o))^+ \in R^{3k \times n_o}$ is the pseudo-inverse matrix of $J_o^T(x_o)$. Substituting (3) into the above equation, we have

$$F_e = -(J_o^T(x_o))^+ (M_o(x_o)\ddot{x}_o + C_o(x_o, \dot{x}_o)\dot{x}_o + G_o(x_o)) \quad (4)$$

Let $x_{ie} \in R^6$ denote the position vector and orientation of the coupling point of the body and ith leg. Then x_{ie} is related to $\dot{q}_i$ and the Jacobian matrix $J_{gi}(q_i)$ in the following way $\dot{x}_{ie} = J_{ie}(q_i)\dot{q}_i$, and the relationship between $\dot{x}_{ie}$ and $\dot{x}_o$ is given by $\dot{x}_{ie} = J_{io}(x_o)\dot{x}_o$. After combining the above equations, the following relationship between the joint velocity of the ith leg and the velocity of the body is obtained $J_{ie}(q_i)\dot{q}_i = J_{io}(x_o)\dot{x}_o$. As it is assumed that the legs work in a nonsingular region, thus the inverse of the Jacobian matrix $J_{ie}(q_i)$ exists. Considering all the legs acting on the body at the same time yields

$$\dot{x}_o = J_o^+(x_o)J_e(q)\dot{q} \quad (5)$$

with $q = [q_1, \ \ldots, \ q_k]^T \in R^{3k}$. Differentiating (5) with respect to time t leads to

$$\ddot{x}_o = J_o^+(x_o)J_e(q)\ddot{q} + \frac{d}{dt}(J_o^+(x_o)J_e(q))\dot{q} \quad (6)$$

Using equations (5) and (6), the dynamics of quadruped robot are then given by

$$M_o(x_o)J_o^+(x_o)J_e(q)\ddot{q} + (M_o(x_o)\frac{d}{dt}(J_o^+(x_o)J_e(q)) + G_o(x_o) + C_o(x_o, \dot{x}_o)J_o^+(x_o)J_e(q))\dot{q} = F_o \quad (7)$$

$$M(q)\ddot{q} + C(q)\dot{q} + G(q) + J_e^T(J_o^T(x_o))^+ F_o = \tau - J_g^T F_g \quad (8)$$

Combining (8) with (7) and multiplying both sides of (8) by $J_o^T(x_o)J_e^T(q)$, the dynamics are given by

$$\mathcal{M}\ddot{q} + \mathcal{C}\dot{q} + \mathcal{G} = \tau - J_g^T F_g \quad (9)$$

where $L = J_o^+(x_o)J_e(q)$, $\mathcal{M} = M(q) + L^T M_o(x_o)L$, $\mathcal{C} = C(q, \dot{q}) + L^T(M_o\dot{L} + C_o(x_o, \dot{x}_o)L)$, $\mathcal{G} = G(q) + L^T G_o(x_o)$.

The dynamic equation (9) has following structure properties, which can be exploited to facilitate the control system design.

III. Formulation of Feet Forces' Distributions

To compute feet forces' distribution, the following assumptions are made:

Assumption III.1. *The legs are assumed to support the trunk body without any slippage at the foot-terrain contact point.*

Assumption III.2. *The contacts of the tips of the leg with ground can be modeled as a shard point contacts with friction, which indicates that the interaction between the tip of the leg and ground is limited to three components of force: one normal and two tangential to the surface.*

For the statically stable walk of a quadruped robot, there are two kinds of supporting phases: three-leg supporting phase and four-leg supporting phase shown in Fig. 1, the quadruped robot in a 3-D workspace with i point contacts between the ground and the legs, fixed with a right-handed coordinate frame. Assume that each leg contacts the ground with Coulomb friction. Let n_i, o_i, and t_i be the unit inward normal and two unit tangent vectors at contact i, where $n_i = o_i \times t_i$. The contact force f_i can be expressed in the local coordinate frame n_i, o_i, t_i by $f_i = [f_{in}, f_{io}, f_{it}]^T$, where f_{in}, f_{io}, and f_{it} are the components of f_i along n_i, o_i, and t_i, respectively.

A contact force f_i is applied by each leg on the ground to hold the quadruped without slippage and tip-over and balance with any external forces. To ensure no slipping at a contact point, with the contact normal along z direction and directed outward and a Coulomb friction coefficient μ_i at contact i, the contact force f_{in} must satisfy the contact constraint $\sqrt{f_{io}^2 + f_{it}^2} \leq \mu f_{in}$, where μ is the static friction coefficient of the substrate. The friction constraint can be geometrically represented as a cone with its axis orthogonal with respect to the support surface and with an "opening angle" equal to $\alpha = \arctan(\mu)$.

In order to overcome the nonlinearities induced by the friction cone equations, it is possible to substitute the friction cone with an inscribed pyramid (see Fig. 1). Hence we have a more restrictive constraint, expressed by $\|f_{io}\| \leq \mu_p f_{in}$, $\|f_{it}\| \leq \mu_p f_{in}$, where $\mu_p = \mu/\sqrt{2}$.

Concerning the adhesion constraint, it can be satisfied if the absolute value of the sum of the distributed forces is less than the maximum allowable friction force, so $f_{io} - \mu_p f_{in} \leq 0$, $-f_{io} - \mu_p f_{in} \leq 0$, $f_{it} - \mu_p f_{in} \leq 0$, $-f_{it} - \mu_p f_{in} \leq 0$, which gives a conservative but linear set of constraints describing a friction pyramid inscribed within the desired friction cone. It is noted that $f_{in} \geq 0$. The friction force constraints may be rewritten as

$$\begin{bmatrix} 1 & 0 & -\mu_p \\ -1 & 0 & -\mu_p \\ 0 & 1 & -\mu_p \\ 0 & -1 & -\mu_p \end{bmatrix} \begin{bmatrix} f_{io} \\ f_{it} \\ f_{in} \end{bmatrix} \leq \begin{bmatrix} 0 \\ 0 \\ 0 \\ 0 \end{bmatrix} \quad (10)$$

We can rewrite the above equation as

$$S_i f_i \leq 0 \quad (11)$$

where S_i is the matrix coefficients of the friction constraints for the ith foot.

The wrench in the global coordinate frame produced by f_i is

$$W_i = G_i f_i \quad (12)$$

where $G_i \in R^{4\times3}$ is the balance matrix for contact i

$$G_i = \begin{bmatrix} n_i & o_i & t_i \\ r_i \times n_i & r_i \times o_i & r_i \times t_i \end{bmatrix} \quad (13)$$

Let $\mathcal{W}_{ext}$ denote the "dynamic" external wrench on the quadruped. For equilibrium, the resultant wrench W_i applied by the feet should always conform to

$$W = \sum_{i=1}^{m} W_i = \sum_{i=1}^{m} G_i f_i = -W_{ext} \quad (14)$$

In real-time control of the balance of the quadruped, W_{ext} is sampled at a sequence of instants with sufficiently small intervals.

Besides the form-closure constraints, to balance any external wrench W_{ext} and maintain a stable balance, we also consider the quadratic objective function of contact forces. So, the optimal contact force with holding the balance can be formulated as the following optimization problem with linear and nonlinear constraints:

$$\text{minimize} \quad J(F_g^d) = \frac{1}{2} F_g^{dT} Q F_g^d + b^T F_g^d \quad (15)$$

$$\text{subject to} \quad G F_g^d = W \quad (16)$$

$$\Phi(F) = S F_g^d \leq 0 \quad (17)$$

$$F_g^d = [f_1, \ldots, f_k]^T \quad (18)$$

where F_g^d is the contact force vector for three-leg support or four-leg support, b is constant, and Q is the symmetric and positive definite matrix with appropriate dimension. The above quadratic object function represents the minimum weighted norm of contact force when $b = 0$.

Considering the Lagrangian function of (15), we obtain

$$\begin{aligned} L(F_g^d, \mu, \lambda) &= F_g^{dT} Q F_g^d + b^T F_g^d \\ &+ \mu^T \Phi(F_g^d) - \lambda^T (G F_g^d - W) \end{aligned} \quad (19)$$

where λ is the Lagrangian multiplier, $\Phi(F_g^d) = [\Phi_1(f_i), \ldots, \Phi_k(f_i)]^T$, and $\Phi_i(f_i) = \sqrt{f_{io}^2 + f_{it}^2} - \mu_p f_{in}$. Let

$$\Psi(F_g^d) = F_g^{dT} Q F_g^d + b^T F_g^d + \mu^{*T} \Phi(F_g^d) \quad (20)$$

$$- \lambda^{*T} (G F_g^d - W) \quad (21)$$

Inspired by [13], we utilize a recurrent neural network, whose dynamics can be given by

$$\begin{bmatrix} \dot{F}_g^d \\ \dot{\mu} \\ \dot{\lambda} \end{bmatrix} = \Lambda \begin{bmatrix} -2QF_g^d - b - \nabla\Phi(F_g^d)\mu + G^T\lambda \\ \max(0, (\mu + \Phi(F_g^d)) - \mu \\ -GF_g^d + W \end{bmatrix} \quad (22)$$

where $F_g^d \in R^{3k}$, $\mu \in R^{4k}$, $\lambda \in R^r$, and Λ is a scaling parameter.

IV. Fuzzy-based motion/force Control

In order to balance the quadruped under external wrench, and avoid the slipping or slippage and tip-over, we can obtain the ground applied constraints force to a desired value F_g^d from (22). Therefore, the constraint force errors $F_g - F_g^d$ should be to be within a small neighborhood of zero, i.e., $\|F_g -$

$F_g^d\| \leq \varsigma$. The second control objective is to design a position control such that the tracking errors of q and $\dot{q}$ from their respective desired trajectories q^d and $\dot{q}^d$ to be within a small neighborhood of zero, i.e., $\|q - q^d\| \leq \varepsilon_1$, and $\|\dot{q} - \dot{q}^d\| \leq \varepsilon_2$. The desired reference trajectory q^d is assumed to be bounded and uniformly continuous, and has bounded and uniformly continuous derivatives up to the second order.

Let $x_i \in R^m$ be the generalized end-effector position vector of the i-th leg, whose relation with the joint configuration variable can be written as $x_i = \Phi_i(q_i)$, where $\Phi_i : \mathbb{R}^\kappa \to \mathbb{R}^l$ is the nonlinear mapping from joint space to task space. The differential kinematics of the i-th leg is

$$\dot{x}_i \quad = \quad J_{gi}(q_i)\dot{q}_i \tag{23}$$

Then, we have the following property.

Property IV.1. *[12] The kinematics (23) is linear with respect to a constant kinematic parameter vector θ_i $\dot{x}_i = J_{gi}(q_i)\dot{q}_i = \mathcal{Z}_i(q_i, \dot{q}_i)\theta_i$, where $\mathcal{Z}_i(q_i, \dot{q}_i)$ is the kinematic regressor matrix. For $x = [x_1, \ldots, x_i, \ldots, x_k]^T$, it is easy to have $\dot{x} = J_g\dot{q} = \mathcal{Z}\theta$, where $J_q = \mathrm{diag}[J_{gi}]$, and $\theta = [\theta_1, \ldots, \theta_i, \ldots, \theta_k]^T$.*

First, let us define a task-space sliding variable $S_i \in R^m$ as $S_i = \dot{e}_i + \Lambda e_i$, where $\Lambda > 0$, and $e_i = x_i - x_i^d$. Next, define a joint-space reference velocity $\dot{q}_i^r \in R^{n-m}$ as

$$\dot{q}_i^r = \hat{J}_{gi}^{-1}(q_i)(\dot{x}_i^d - \Lambda e_i) \tag{24}$$

where $\hat{J}_{gi}$ is the estimation of J_{gi}. Let $\dot{q}^r = [\dot{q}_1^r, \ldots, \dot{q}_k^r]^T$, a joint-space sliding vector $s_{jh} \in R^n$ can be defined as $s_i = \dot{q}_i - \dot{q}_i^r$, so, the relation between S_i and s_i can be described as

$$S_i \quad = \quad \hat{J}_{gi}s_i - \mathcal{Z}_i\tilde{\theta}_i \tag{25}$$

where $\tilde{\theta}_i = \hat{\theta}_i - \theta_i$. Let $S = [S_1, \ldots, S_k]^T$, and $s = [s_1, \ldots, s_k]^T$, integrating (9), the closed-loop dynamics can be presented as

$$\mathcal{M}\dot{s} + \mathcal{C}s \quad = \quad \tau - \Xi - J_g^T F_g \tag{26}$$

where $\Xi = \mathcal{M}\ddot{q}^r + \mathcal{C}\dot{q}^r + \mathcal{G}$.

According to the universal approximation theorem, it can be approximated by a multiple-input-multiple-output (MIMO) fuzzy logic system $\hat{\Xi}(\ddot{q}^r, \dot{q}^r, q|\Theta)$, which can be described as $\hat{\Xi}(\ddot{q}^r, \dot{q}^r, q|\Theta) = [\hat{\Xi}_1(\ddot{q}_1^r, \dot{q}_1^r, q_1|\Theta_1), \cdots, \hat{\Xi}_k, \cdots,$ $\hat{\Xi}_{(3k}(\ddot{q}_{3k}^r, \dot{q}_{3k}^r, q_{3k})|\Theta_{3k})]^T$, where $\hat{\Xi}_j(\ddot{q}_j^r, \dot{q}_j^r, q_j|\Theta_j) = \Theta_j^T\xi_j(x_j)$, the vector $\xi_j(x_j)$ is known as the fuzzy basis function vector, and the input vector to the FLS is $x_j = [\ddot{q}_j^r, \dot{q}_j^r, q_j]^T$ and Θ_j is the jth column of matrix Θ_j. Note that the input vector x_j is composed of 3 elements, the total number of fuzzy rules, in the FLS of each robot is 3^ν . It is usually a very large number and would consume a great amount of computational resources.

To reduce the total number of fuzzy rules required even further, we adopt a decomposition procedure to partition the function into three different functions. Nominally

$$\Xi_j(\ddot{q}_j^r, \dot{q}_j^r, q_j) = \Xi_j^1(\ddot{q}_j^r, q_j) + \Xi_j^2(\dot{q}_j^r, q_j) \tag{27}$$

Similarly, its approximated value generated by the MIMO-FLS is expressed as

$$\hat{\Xi}_j \quad = \quad \hat{\Xi}_j^1 + \hat{\Xi}_j^2 \tag{28}$$

where $\hat{\Theta}_j = [\hat{\Theta}_j^{1T}, \hat{\Theta}_j^{2T}]^T$ is the estimation of Θ_j, $\hat{\Xi}_j^1(\ddot{q}_j^r, q_j|\Theta_j^1) = (\hat{\Theta}_j^1)^T\xi_j^1(\ddot{q}_j^r, q_j)$, $\hat{\Xi}_j^2(\dot{q}_j^r, q_j|\Theta_j^2) = (\hat{\Theta}_j^2)^T\xi_j^2(\dot{q}_j^r, q_j)$.

Then, we can define the consequent parameter matrices adaptation for the three fuzzy logic components of the FLS as

$$\dot{\hat{\Theta}}_j^1 = (\Gamma_j^1)\xi_j^1(\ddot{q}_j^r, q_j)s_j^T \tag{29}$$

$$\dot{\hat{\Theta}}_j^2 = (\Gamma_j^2)\xi_j^2(\dot{q}_j^r, q_j)s_j^T \tag{30}$$

where Γ_j^1, Γ_j^2 are positive definite gains. Through this fuzzy rule reduction technique, the total number of rules drops down to $3(\nu)^{2\nu}$, which need be fired by the three fuzzy logic components of the FLS at each robot. This is a significant decrease of computational consume compared to the original number, which would facilitate its real-world implementation.

Since the foot tip is constrained by environment, the force F_g is exerted to the foot tip at the contact point, a new concept of Jacobian estimation can be introduced as force projection error

$$e_J = \tilde{J}_g^T(q)F_g = \hat{J}_g^T F_g - J_g^T(q)F_g \tag{31}$$

which is also a measure of mismatch between $\hat{J}_g$ and J_g and it can be calculated from measurements. The force projection error is measured through using force signal, which indicates that for identification of constraining surface geometry, force signal is more informative.

Define the tracking control $\dot{\hat{e}} = \dot{\hat{x}} - \dot{x}^d$ and $\hat{S} = \dot{\hat{e}} + \Lambda e$. Then, we proposed the following adaptive cooperative tracking control to compensate the dynamical uncertainties, which are defined as follows:

$$\begin{aligned}\tau \quad = \quad & -\hat{J}_g^T(q)K_x\hat{S} - \mathrm{sgn}(s)\hat{\Xi} + \hat{J}_g^T(q)F_g^d \\ & -\hat{J}_g^T(q)e_f + K_f e_J\end{aligned} \tag{32}$$

where $\mathrm{sgn}(s) = [\mathrm{sgn}(s_1), \ldots, \mathrm{sgn}(s_j), \ldots, \mathrm{sgn}(s_n)]$, and $\mathrm{sgn}(s_j) = \frac{s_j}{\|s_j\|}$, $e_f = F_g^d - F_g$, and K_x and K_f are positive diagonal and satisfying $K_x > \frac{1}{2}$.

In the adaptive control law (32), the first term $-\hat{J}_g^T(q)K_x\hat{S}$ is an approximate transpose Jacobian feedback of the task space velocities and position errors, the second term is an estimated dynamic compensation, and the third term is the estimated Jacobian error term through the force control. Updating the estimated dynamic parameters $\hat{\theta}_j$ using (29) and (30), the closed-loop dynamics can be obtained by substituting (32) into (26):

$$\begin{aligned}\mathcal{M}\dot{s} + \mathcal{C}s \quad = \quad & -\hat{J}_g^T(q)K_x\hat{S} - \mathrm{sgn}(s)\hat{\Xi} \\ & -\Xi + \tilde{J}_g^T F_g + K_f e_J\end{aligned} \tag{33}$$

where $\tilde{\Theta} = \hat{\Theta} - \Theta$ is the dynamic parameter estimation error and $\tilde{J}_g = \hat{J}_g(q) - J_g(q)$. Multiplying both sides of the above equation using s^T, we get

$$s^T[\mathcal{M}\dot{s}+\mathcal{C}s] = -s^T\hat{J_g}^T(q)K_x\hat{S} - s^T\text{sgn}(s)\hat{\Xi} - s^T\Xi + s^T\tilde{J}_g^TF_g + s^TK_fe_J \quad (34)$$

Define the Lyapunov function candidate as

$$V = \frac{1}{2}s^T\mathcal{M}s + \frac{1}{2}\tilde{\Theta}^T\Gamma^{-1}\tilde{\Theta} + \frac{1}{2}\tilde{\theta}^T\Omega^{-1}\tilde{\theta} \quad (35)$$

where $\tilde{\Theta} = \hat{\Theta} - \Theta$, and $\tilde{\theta} = \hat{\theta} - \theta$, and $\Gamma = \text{diag}[\Gamma^1, \Gamma^2]$.

Consider the derivative of V as

$$\dot{V} = \frac{1}{2}s^T(2\mathcal{M}\dot{s} + \dot{\mathcal{M}}s) + \tilde{\Theta}^T\Gamma^{-1}\dot{\tilde{\Theta}} + \tilde{\theta}^T\Omega^{-1}\dot{\tilde{\theta}} \quad (36)$$

Using the skew symmetry of $s^T(\dot{\mathcal{M}} - 2\mathcal{C})s = 0$, we can obtain the derivative of $\dot{V}$ as

$$\dot{V} = -s^T\text{sgn}(s)\hat{\Xi} - s^T\hat{J}_g^T(q)K_x\hat{S} - s^T\Xi + s^T\tilde{J}_g^TF_g + s^TK_fe_J + \tilde{\Theta}^T\Gamma^{-1}\dot{\tilde{\Theta}} + \tilde{\theta}^T\Omega^{-1}\dot{\tilde{\theta}} \quad (37)$$

Then, we have

$$\dot{V} \leq -\sum_{j=1}^{3k}(\|s_j\|(\tilde{\Theta}_j^1)^T\xi_j^1(\ddot{q}_j^r, q_j) + \|s_j\|(\tilde{\Theta}_j^2)^T\xi_j^2(\ddot{q}_j^r, q_j)) - s^T\hat{J}_g^T(q)K_x\hat{S} + s^T\tilde{J}_g^TF_g + s^TK_fe_J + \tilde{\theta}^T\Omega^{-1}\dot{\tilde{\theta}} + \tilde{\Theta}^T\Gamma^{-1}\dot{\tilde{\Theta}} \quad (38)$$

Considering (25), we have

$$\hat{J}_gs = S + \mathcal{Z}\tilde{\theta} \quad (39)$$

moreover $\hat{S} = \mathcal{Z}\tilde{\theta} + S$. Therefore, we have $\hat{J}_gs = \hat{S}$. Integrating (29) and (30), substituting (39) into (38), we have

$$\dot{V} \leq -\hat{S}^TK_x\hat{S} + s^T\tilde{\theta}^T\mathcal{Z}^TF_g + s^TK_f\mathcal{Z}\tilde{\theta}F_g + \tilde{\theta}^T\Omega^{-1}\dot{\tilde{\theta}} \quad (40)$$

We choose the following adaptive law as

$$\dot{\hat{\theta}}_i = -\omega_i\mathcal{Z}_i^T(K_f+1)F_gs \quad (41)$$

where $\omega_i > 0$. Integrating (41) into (40) we have

$$\dot{V} \leq -\hat{S}^TK_x\hat{S} \leq 0 \quad (42)$$

Theorem IV.1. *Consider the dynamics of quadruped robot (1), and furthermore the approximate Jacobian $\hat{J}_{gi}(q_i)$ is non-singular, the adaptive controller (32) combining the adaptive law (29), (30) and (41) will ensure both the convergence of the task-space tracking errors, namely, $x_i \to x_i^d$, $\dot{x}_i \to \dot{x}_i^d$, and $F_g \to F_g^d$ as $t \to \infty$.*

Proof: Since $\dot{V} \leq 0$, V must be bounded, resulting in the boundedness of s_i, $\tilde{\Theta}$, $\tilde{\theta}_i$. From Eq. (24), we have $q_i^r \in L_\infty$ since the approximate Jacobian $J_{gi}(q_i)$ has full rank. Thus $\dot{q}_i = s_i + \dot{q}_i^r \in L_\infty$, implying that $\dot{x}_i \in L_\infty$. Therefore, we obtain $\dot{\hat{\theta}}_i \in L_\infty$ based on (41). From the closed-loop dynamics (26), we obtain $\dot{s}_i \in L_\infty$ and thus $\ddot{q}_i \in L_\infty$, $\ddot{x}_i \in L_\infty$. Based on the result (42), we conclude that V is uniformly continuous. Using Barbalats Lemma [11], we derive the result that $\dot{V} \to 0$ as $t \to \infty$, which gives rise to the result that $s_i \to 0$, $\hat{S} \to 0$ and $\tilde{\theta} \to 0$, then $x_i \to x_i^d$, $\dot{x}_i \to \dot{x}_i^d$, and $F_g \to F_g^d$ as $t \to \infty$. ■

V. Simulation Studies

In the simulation, the system parameters are chosen as $m_1 = 0.45kg$,$L_1 = 0.4m$, $m_2 = 1.74kg$, $L_2 = 1m$, $m_3 = 1.3kg$, $L_3 = 1m$, $g = 9.8m/s^2$, $I_{1zz} = 0.018kgm^2$, $I_{2zz} = 0.735kgm^2$, $I_{3zz} = 0.549kgm^2$, $I_{2xx} = 0.435kgm^2$, $I_{3xx} = 0.325kgm^2$. We assume the lower limit and the upper limit of each foot friction $f_i = [f_{io}, f_{it}, f_{in}]^T$ is $[-30, -30, -100]^T$ and $[30, 30, 100]^T$ separately, and $Q = \text{diag}[1.0]$, $b = 0$. The friction coefficient of each leg is $\mu = 0.6$. The external forward perturbation force is $f_{ext} = 15\sin(2\pi t)N$ at $d = 1m$ height of the middle body-platform rear, as shown in Fig. 1. Some matrices going to be used in the simulation are set as $G = \begin{bmatrix} 1 & 0 & 0 & -1 & 0 & 0 & 1 & 0 & 0 & -1 & 0 & 0 \\ 0 & 1 & 0 & 0 & 1 & 0 & 0 & 1 & 0 & 0 & 1 & 0 \\ 0 & 0 & 1 & 0 & 0 & 1 & 0 & 0 & 1 & 0 & 0 & 1 \\ 0 & 0 & 0.25 & 0 & 0 & 0.25 & 0 & 0 & 0.25 & 0 & 0 & 0.25 \end{bmatrix}$, $S_i = \begin{bmatrix} 1 & 0 & -0.424 \\ -1 & 0 & -0.424 \\ 0 & 1 & -0.424 \\ 0 & -1 & -0.424 \end{bmatrix}$, $f = [f_{1o}, f_{1t}, f_{1n}, f_{2o}, f_{2t}, f_{2n}, f_{3o}, f_{3t}, f_{3n}, f_{4o}, f_{4t}, f_{4n}]^T$, $W = [0, f_{ext}, G_q, f_{ext}d]^T$, where S_i is the matrix coefficients of the friction constraints for ith foot, G_q is the gravity of the quadruped robot. The fuzzy logic control without any knowledge of system dynamics is employed as below. The adaptive update parameters are chosen as $\Gamma_1 = 100$, $\Gamma_2 = 100$ and $\Omega = diag[10]$. Other parameters are defined as, $K_f = diag[10]$, $K_x = diag[150]$ and $\Lambda = 100$.

The simulation results of the quadruped are shown in Figs. 2–9. Figs. 2–3 show the optimized decomposed forces of the four legs. The solid lines represent the computed tangential and inward components (f_o,f_t,f_n), and the dotted lines represent the measured components (f_o, f_t, f_n) correspondingly. Figs. 4–5 show the tracking errors of the joint positions of all the four legs. Figs. 6–7 show the velocities for all the four legs. The input torques for all the four legs are shown in Figs. 8–9. As illustrated by the simulation results, that the trajectory tracking errors and force tracking errors are bounded within a small value, which validate the effectiveness of the control law in Theorem IV.1.

VI. Conclusions

In this paper, the dynamic balance optimization and control of quadruped robots have been investigated under external disturbances. A gradient neural network is adopted to minimize this quadratic objective function with respect to linear equality and inequality constraints. Then, hybrid motion/force control based on adaptive neural network is proposed to compensate for the external perturbation in the environment

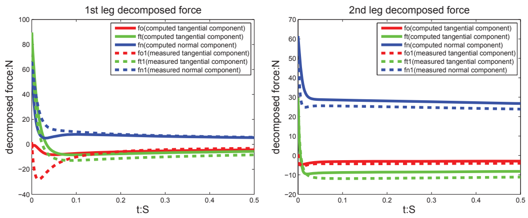

Fig. 2: Decomposed forces for 1^{st} and 2^{nd} legs

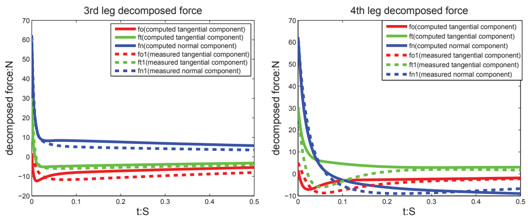

Fig. 3: Decomposed forces for 3^{rd} and 4^{th} legs

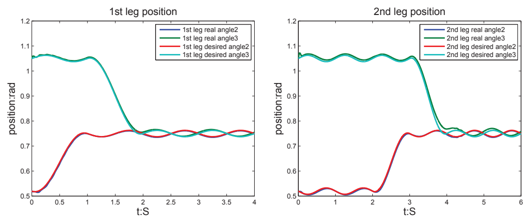

Fig. 4: Joint angle trajectories of 1^{st} and 2^{nd} legs

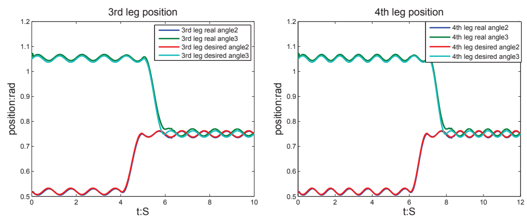

Fig. 5: Joint angle trajectories of 3^{rd} and 4^{th} legs

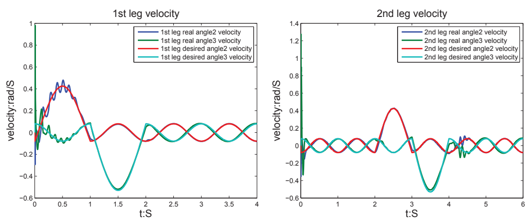

Fig. 6: Joint angle velocities of 1^{st} and 2^{nd} legs

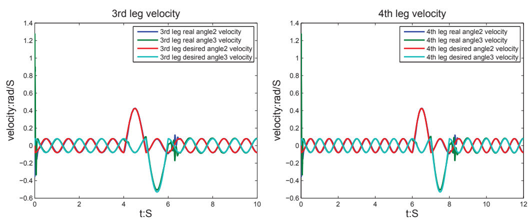

Fig. 7: Joint angle velocities of 3^{rd} and 4^{th} legs

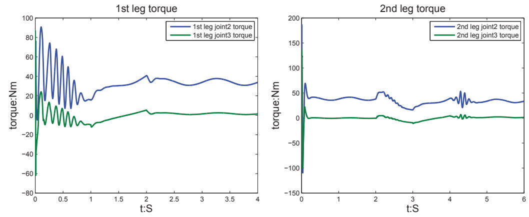

Fig. 8: Torque inputs for 1^{st} and 2^{nd} legs

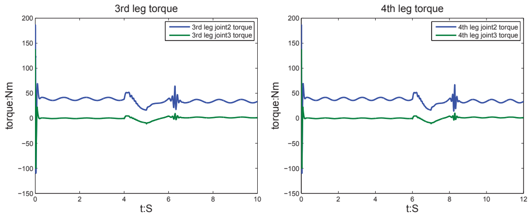

Fig. 9: Torque inputs for 3^{rd} and 4^{th} legs

and approximate feedforward force and impedance of the leg joints on line.

REFERENCES

[1] M. S. Erden and K. Leblebicioglu, "Torque distribution in a six-Legged robot", *IEEE Trans. Robotics*, vol. 23, no. 1, Feb. 2007, pp. 179–186.

[2] D. C. Kar, K. K. Issac, K. Jayarajan, " Minimum energy force distribution for a walking robot", *Journal of Robotic Systems* , vol. 18, no. 2, 2001, pp. 47–54.

[3] M. Fujiata and H. Kitano, "Development of an autonomous quadruped robot for robot entertainment", *Autonomous Robots*, vol. 5, pp. 7–18, 1998.

[4] M. Raibert, K. Blankespoor, G. Nelson, R. Playter, " BigDog, the rough-terrain quadruped robot," *Proceedings of the 17th World Congress*, Seoul, Korea, July 6-11, 2008, pp. 10822–10825.

[5] M. Kalakrishnan, J. Buchli, P. Pastor, M. Mistry, S. Schaal, "Fast, robust quadruped locomotion over challenging terrain," *20d10 IEEE International Conference on Robotics and Automation*, 2010, pp. 2665–2670.

[6] P. Yin, P. Wang, M. Li, L. Sun, "A novel control strategy for quadruped robot walking over irregular terrain", *IEEE Conference on Robotics, Automation and Mechatronics*, 2011 , pp. 184–189.

[7] S. S. Roya, D. K. Pratihar, "Effects of turning gait parameters on energy consumption and stability of a six-legged walking robot", *Robotics and Autonomous Systems*, vol. 60, 2012, pp. 72–82.

[8] X. Chen, K. Watanabe, K. Kiguchi, and K. Izumi, "Optimal force distribution for the legs of a quadruped robot", *Machine Intelligence & Robotic Control*, vol. 1, no. 2, pp. 87–94, 1999.

[9] Y. Zheng, C. M. Chew, A. H. Adiwahono, " GJK-based approach to contact force feasibility and distribution for multi-contact robots," *Robotics and Autonomous Systems*, vol. 59, 2011, pp. 194–207.

[10] M. S. Bazaraa, H. D. Sherali, and C. M. Shetty, *Nonlinear Programming Theory and Algorithms*, 2nd ed. New York: Wiley, 1993.

[11] S. S. Ge, T. H. Lee, and C. J. Harris, *Adaptive neural network control of robot manipulators*, World Scientific, London, 1998.

[12] Z. Li, S. S. Ge, M. Adams, W. S. Wijesoma, "Robust adaptive control of uncertain force/motion Constrained Nonholonomic Mobile Manipulators," *Automatica*, vol. 44, no. 3, 2008, pp. 776-784.

[13] Y. Xia, J. Wang, and L. Fo, "Grasping-Force Optimization for Multifingered Robotic Hands Using a Recurrent Neural Network," *IEEE Trans. Robotics and Automation*, vol. 20, no. 3, JUNE 2004, pp. 549–554.